nature climate change

ARTICLES

https://doi.org/10.1038/s41558-022-01391-9

Check for updates

OPEN

Mangrove dispersal disrupted by projected changes in global seawater density

Tom Van der Stocken[1,2] ✉, Bram Vanschoenwinkel[1], Dustin Carroll[2,3], Kyle C. Cavanaugh[4] and Nico Koedam[1]

The degree to which the distribution of mangrove forests will be impacted by climate change depends on the dispersal and establishment of sea-faring propagules, which drive forest rejuvenation, gene flow and range expansion. Climate change affects sea surface density via changes in temperature and salinity. However, these changes have not been mapped and it remains unclear how these factors may impact mangrove propagule dispersal. Here, we provide evidence for strong warming of coastal mangrove waters and elevated geographic variability in surface ocean density under representative concentration pathway RCP 8.5 by 2100. The largest changes will occur in the Indo West Pacific region, the primary hotspot of mangrove diversity. By comparing propagule densities to predicted sea surface density, we assessed potential effects on mangrove propagule dispersal. In the future, a warmer and fresher ocean is likely to alter dispersal trajectories of mangrove propagules and increase rates of sinking in unsuitable offshore locations, potentially reducing the resilience of mangrove forests.

Mangrove forests thrive along tropical and subtropical shorelines and their distribution extends to warm temperate regions[1]. They are globally recognized for the valuable ecosystem services they provide[2] but are expected to be substantially influenced by climate change-related physical processes in the future[3,4]. Under warming winter temperatures, poleward expansion is predicted for mangroves[5,6], with potential implications for ecosystem structure and functioning, as well as human livelihoods and well-being[7,8]. The global distribution, abundance and species richness of mangroves is governed by a broad range of biotic and environmental factors, including temperature and precipitation[9] and diverse geomorphological and hydrological gradients[10]. Climate and aspects related to coastal geography (for example, floodplain area) determine the availability of suitable habitat for establishment[11,12]. However, the potential for mangroves to track changing environmental conditions and expand their distributions ultimately depends on dispersal[11,13]. The importance of dispersal in controlling mangrove distributions has been demonstrated by mangrove distributional responses to historical climate variability[14], past mangrove (re) colonization of oceanic islands[15] and from the long-term survival of mangrove seedlings planted beyond natural range limits[16]. As such, quantifying changes in the factors that influence dispersal is important for understanding climate-driven distributional responses of mangroves under future climate conditions.

In mangroves, dispersal is accomplished by buoyant seeds and fruits (hereafter referred to as 'propagules'). In combination with prevailing currents, the spatial scale of this process, ranging from local retention to transoceanic dispersal over thousands of kilometres[13], is determined by propagule buoyancy[17], that is, the density difference between that of propagules and the surrounding water. Hence, the course of dispersal trajectories for propagules from these species depends on the interaction between spatiotemporal changes in both propagule density and that of the surrounding water, rendering this process sensitive to climate-driven changes in coastal and open-ocean water properties. The biogeographic implications of such density differences were recognized more than a century ago by Henry Brougham Guppy, who discussed[18] 'the far-reaching influence on plant-distribution and on plant-development that the relation between the specific weight of seeds and fruits and the density of sea-water must possess'.

Since the time of Guppy's early observations, climate change from human activities has driven pronounced changes in ocean temperature and salinity, with further changes predicted throughout the twenty-first century[19]. Ocean density is a nonlinear function of temperature, salinity and pressure[20]; therefore, these changes may influence dispersal patterns of mangrove propagules by altering their buoyancy and floating orientation. As Guppy noted[18], '[for] plants whose seeds or fruits are not much lighter than sea-water […] the effect of increased density of the water is to extend the flotation period' or 'to increase the number that floated for a given period'. Guppy also reported that the seedlings of the widespread mangrove genera *Rhizophora* and *Bruguiera* present exceptional examples of propagules with densities somewhere between seawater and freshwater[18]. Previous studies of the impacts of climate change on mangroves have focused on factors such as sea level rise, altered precipitation regimes and increasing temperature and storm frequency[4,21–23] but the potential impact of climate-driven changes in seawater properties on mangroves has not yet been examined. This is somewhat surprising, as the ocean is the primary dispersal medium of this 'sea-faring' coastal vegetation and dispersal is a key process that governs a species' response to climate change by changing its geographical range. This knowledge gap contrasts with recent efforts to expose links between climate change and dispersal in other ecologically important marine taxa such as zooplankton and fish species[24–27].

In this study, we investigate predicted changes in sea surface temperature (SST), sea surface salinity (SSS) and sea surface density (SSD) for coastal waters bordering mangrove forests (hereafter referred to as 'coastal mangrove waters'), over the next century.

[1]Department of Biology, Vrije Universiteit Brussel, Brussels, Belgium. [2]Earth Science Section, Jet Propulsion Laboratory, California Institute of Technology, Pasadena, CA, USA. [3]Moss Landing Marine Laboratories, San José State University, Moss Landing, CA, USA. [4]Department of Geography, University of California, Los Angeles, CA, USA. ✉e-mail: Tom.Van.Der.Stocken@vub.be

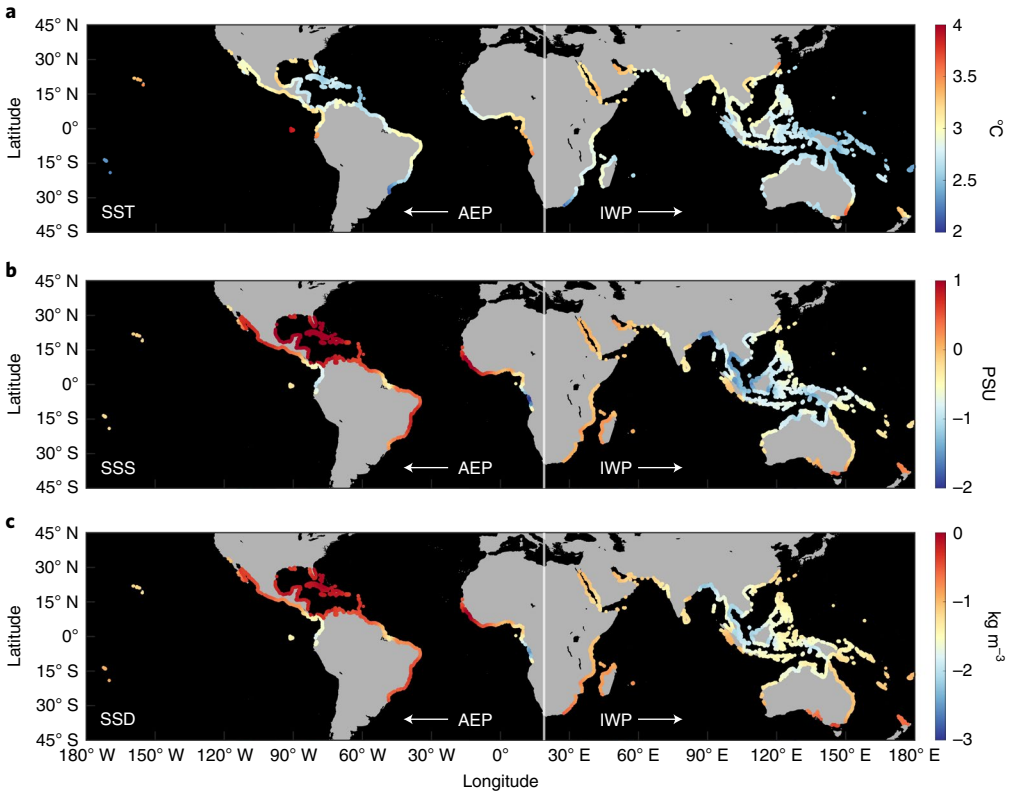

Fig. 1 | Global map showing the change in sea surface variables across mangrove bioregions under RCP 8.5. a–c, Change in SST (**a**), SSS (**b**) and SSD (**c**). Changes in SST and SSS are based on present-day (2000–2014) and future (2090–2100) marine fields from the Bio-ORACLE database[29,30], from which SSD data were derived. The vertical line (19° E) separates the two major mangrove bioregions: the AEP and IWP.

Using a biogeographic classification system for coastal and shelf areas[28], we examine spatiotemporal changes in these surface ocean properties, with a particular focus on the world's two major mangrove diversity hotspots: (1) the Atlantic East Pacific (AEP) region, including all of the Americas, West and Central Africa and (2) the Indo West Pacific (IWP) region, extending from East Africa eastwards to the islands of the central Pacific[1]. Finally, we synthesize available data on the density of mangrove propagules for different mangrove species and explore the potential impact of climate-driven changes in SSD on propagule dispersal.

To assess changes in SST and SSS throughout the global range of mangrove forests, we used present (2000–2014) and future (2090–2100) surface ocean properties from the Bio-ORACLE database[29,30]. SSD estimates were derived from these variables using the UNESCO EOS-80 equation of state polynomial for seawater[31]. Changes in SST, SSS and SSD (Fig. 1) were calculated for four representative concentration pathways (RCPs) and derived for coastal waters closest to the 583,578 polygon centroids from the 2015 Global Mangrove Watch (GMW) database[32]. After removing duplicates, our dataset contained 10,108 unique mangrove occurrence locations, with corresponding present conditions and predicted future changes in mean SST, SSS and SSD. Under the low-warming scenario RCP 2.6, mean SST of coastal mangrove waters is predicted to change by +0.64 (±0.11) °C and mean SSS by −0.06 (±0.25) practical salinity units (PSU). Combined, this results in an average change in mean SSD of −0.25 (±0.20) kg m^{-3} in coastal mangrove waters by the late twenty-first century (Supplementary Table 1). These values roughly double under RCP 4.5 (Supplementary Table 2), while under RCP 6.0, a change of +1.69 (±0.14) °C in mean SST, −0.21 (±0.42) PSU in mean SSS and −0.71 (±0.32) kg m^{-3} in mean SSD is predicted (Supplementary Table 3). Under RCP 8.5, our study predicts a change in SST of +2.84 (±0.21) °C (range 2.11–4.01 °C), a change in SSS of −0.30 (±0.74) PSU (−2.01–1.26 PSU) and a corresponding change in SSD of −1.17 (±0.56) kg m^{-3} (−2.53–0.03 kg m^{-3}) (Supplementary Table 4).

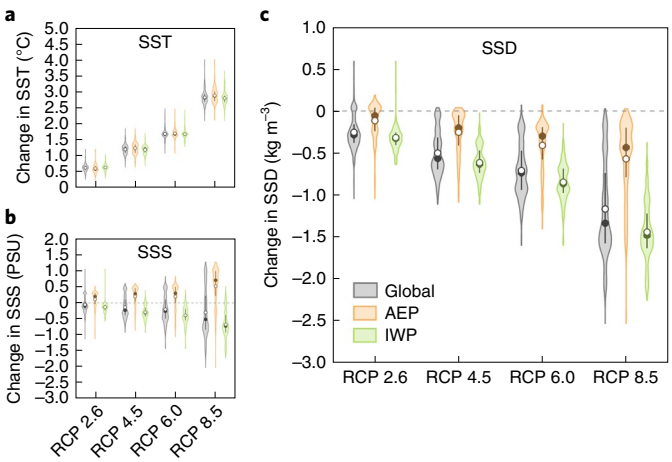

Fig. 2 | Change in surface ocean properties for coastal waters bordering mangrove forests and in the two major mangrove bioregions, the AEP and IWP, for different RCPs. a–c, Variation in SST (**a**), SSS (**b**) and SSD (**c**) under various RCP scenarios. Grey indicates global distribution (n = 10,108), orange denotes AEP (n = 3,190) and green represents IWP (n = 6,918). Data for SST and SSS consist of present-day (2000–2014) and future (2090–2100) marine fields from the Bio-ORACLE database[29,30], from which SSD data were derived. The cat-eye plots[50] show the distribution of the data. Median and mean values are indicated with black and white circles, respectively, and the vertical lines represent the interquartile range.

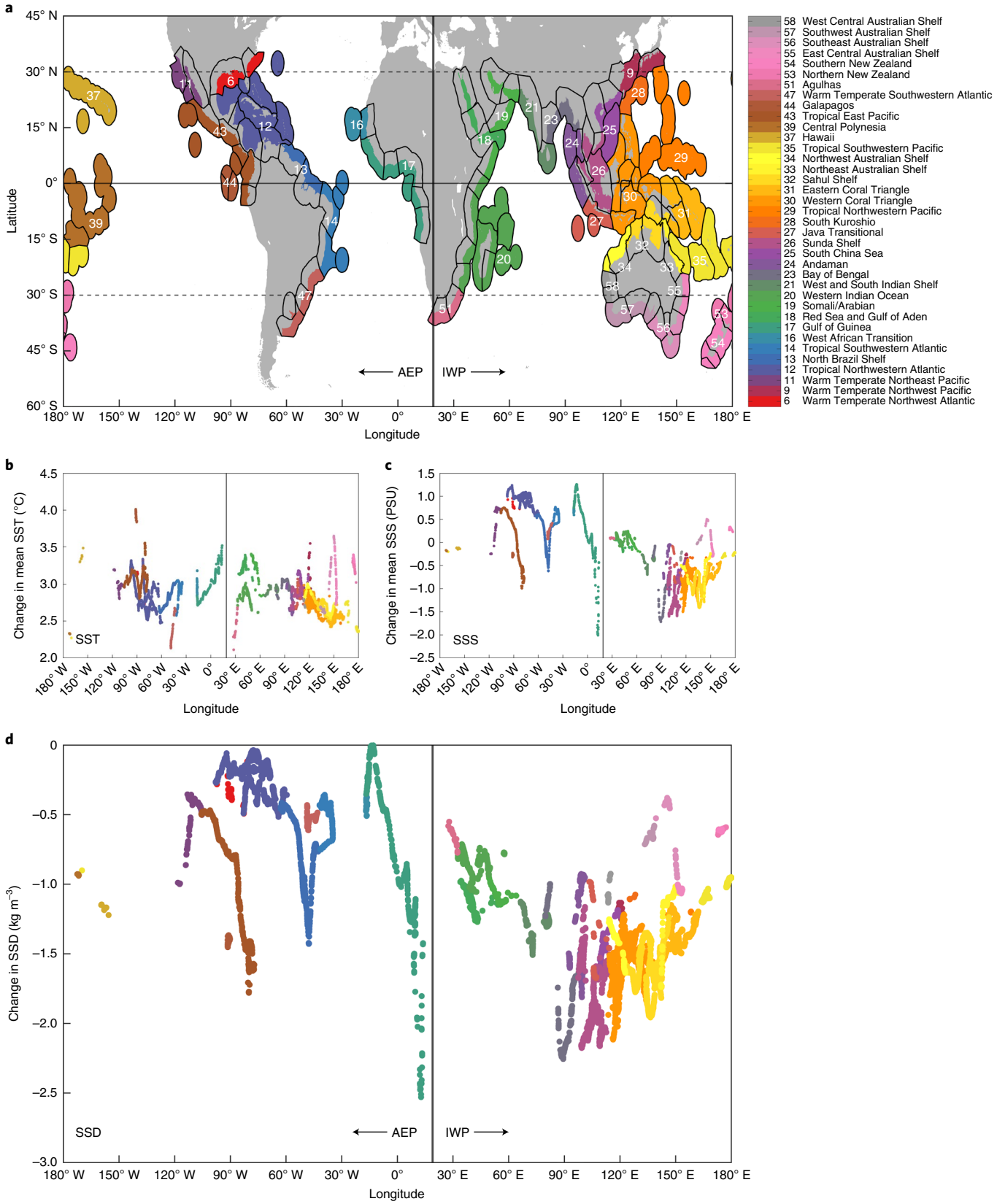

Fig. 3 | Global spatial variability in SST, SSS and SSD for coastal waters bordering mangrove forests under RCP 8.5. a, Global map showing the provinces (colour code and numbers) from the MEOW database[28] used to investigate spatial patterns in mangrove coastal ocean water changes by 2100. **b**–**d**, Longitudinal gradient of the change in SST (**b**), SSS (**c**) and SSD (**d**) under RCP 8.5 in the AEP and the IWP mangrove bioregions; circles are coloured according to the MEOW province in which respective mangrove sites are located.

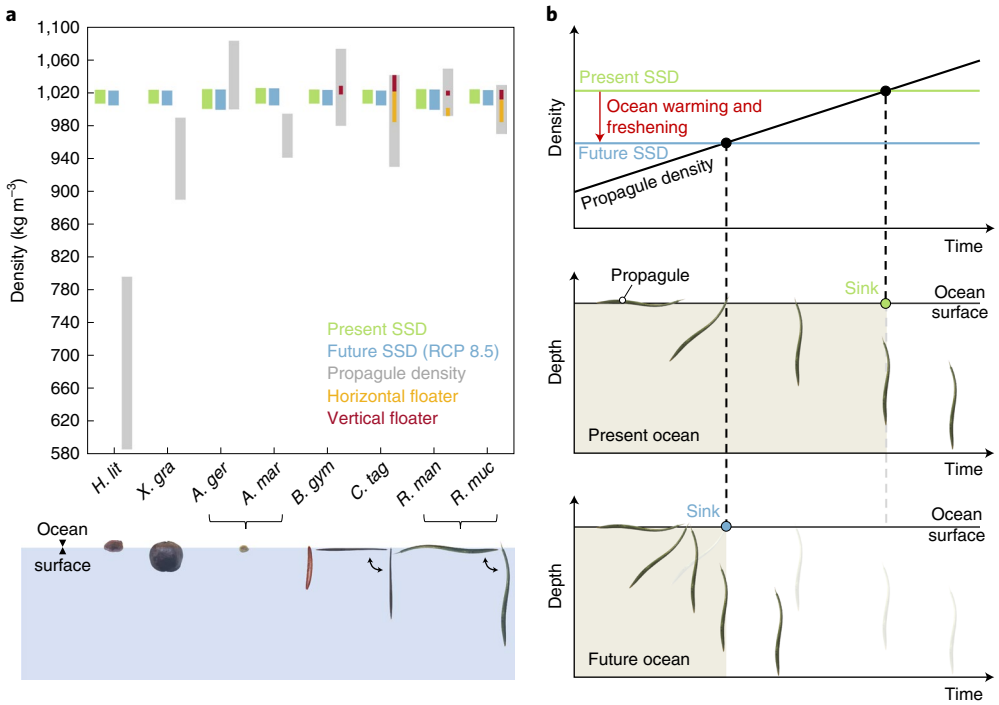

Fig. 4 | Potential effect of future declines in SSD on mangrove propagule dispersal. a, Range of reported propagule density values for wide-ranging mangrove species and present and future range of SSD for coastal waters along the range of those mangrove species. Mangrove propagule data are extracted from the literature (Supplementary Table 5). *H. lit*, *Heritiera littoralis*; *X. gra*, *Xylocarpus granatum*; *A. ger*, *Avicennia germinans*; *A. mar*, *Avicennia marina*; *B. gym*, *Bruguiera gymnorrhiza*; *C. tag*, *Ceriops tagal*; *R. man*, *Rhizophora mangle*; *R. muc*, *Rhizophora mucronata*. Bottom part adapted from ref. [51]. **b**, Conceptual figure of the potential effects of ocean warming and freshening on mangrove propagule dispersal. Ocean warming and freshening drive changes in SSD and may reduce the timeframe for opportunistic colonization. For a propagule with a specific density and floating profile under present surface ocean conditions, reduced SSD of coastal and open-ocean waters may reduce floatation time (shaded area) and hence, reduce the proportion of long-distance dispersers. For simplicity, the density of propagules is assumed to increase linearly over time, although the actual increase may be nonlinear.

Spatial variability in predicted surface ocean property changes was examined by considering the two major mangrove bioregions (AEP and IWP) (Fig. 2) and using the Marine Ecoregions of the World (MEOW) biogeographic classification[28] (Fig. 3). Both the range and changes in mean SST were comparable for the AEP and IWP mangrove bioregions, for all respective RCP scenarios (Fig. 2a and Supplementary Tables 1–4). Under RCP 8.5, mean SST in both mangrove bioregions is predicted to warm ~2.8 °C by 2100, which is roughly 4.5 times the predicted increase in mean SST under RCP 2.6 (Supplementary Tables 1 and 4). Predictions for the RCP 8.5 scenario are generally consistent with reported global ocean temperature trends[33] and show that the greatest warming occurs in coastal waters near the Galapagos Islands (change in mean SST of 3.92 ± 0.06 °C). Pronounced SST increases are also predicted for Hawaii (change in mean SST of 3.36 ± 0.05 °C), the Southeast Australian Shelf (3.30 ± 0.25 °C), Northern and Southern New Zealand (3.25 ± 0.07 °C and 3.34 ± 0.02 °C, respectively), Warm Temperate Northwest Pacific (3.27 ± 0.16 °C), the Red Sea and Gulf of Aden (3.24 ± 0.08 °C), Somali/Arabian Coast (3.23 ± 0.15 °C), South China Sea (3.07 ± 0.10 °C), the Tropical East Pacific (3.09 ± 0.15 °C) and the Warm Temperate Northwest Atlantic (3.14 ± 0.13 °C) (Fig. 3b and Supplementary Tables 4).

Predicted SSS changes exhibit an opposite trend in the AEP and IWP bioregions, with increased salinity in the AEP and reduced salinity in the IWP under global warming (RCP 2.6–RCP 8.5; Fig. 2b); this is reflected in contrasting SSD changes in both mangrove bioregions (Fig. 2c) and associated with predicted global changes in precipitation, with extensions of the rainy season over most of the monsoon domains, except for the American monsoon[34]. Under RCP 8.5, the spatially averaged change in mean SSS is +0.51 (±0.57) PSU in the AEP and −0.68 (±0.44) PSU in the IWP region. The maximum decrease in mean SSS (−2.01 PSU) is predicted for the Gulf of Guinea in the AEP bioregion (Fig. 3c and Supplementary Table 4). Within the IWP, the Western Indian Ocean region shows little or no changes in SSS, which contrasts with the pronounced freshening trends predicted in the eastern part of this ocean basin and the Tropical West Pacific (Figs. 1b and 3c). Increased freshening is predicted in the Bay of Bengal (SSS change: −1.17 ± 0.43 PSU), the Sunda Shelf (SSS change: −1.21 ± 0.29 PSU) and the Western Coral Triangle province (mean SSS change: −0.80 ± 0.17 PSU) (Fig. 3c and Supplementary Table 4). Within the AEP, salinity increases exceed +0.96 PSU in the Tropical Northwestern Atlantic, +0.80 in the Warm Temperate Northwest Atlantic and +0.68 in the West African Transition (Fig. 3c and Supplementary Table 4). The spatial heterogeneity in SSS across the global range of mangrove forests corresponds with observed changes in SSS[35]. Trends in SSD (Fig. 3d) strongly track changes in SSS (Fig. 3c) rather than SST. All RCP scenarios predict an overall decrease in SSD for both mangrove bioregions; however, the predicted decrease in SSD in the IWP region was a factor of 2 (RCP 6.0) and 2.5 (RCP 2.6, RCP 4.5 and RCP 8.5) stronger than in the AEP (Figs. 2 and 3d and Supplementary Tables 1–4).

Propagule density values from our literature survey range from <600 kg m^{-3} to >1,080 kg m^{-3} for different mangrove species (Fig. 4 and Supplementary Table 5). The low densities reported for *Heritiera littoralis* propagules provide a strong contrast with the near-seawater propagule densities reported for *Avicennia* and members of the Rhizophoraceae (*Bruguiera*, *Rhizophora* and *Ceriops*). Floating characteristics of the latter may be particularly sensitive to changes in SSD. To illustrate the potential influence of changing ocean conditions on

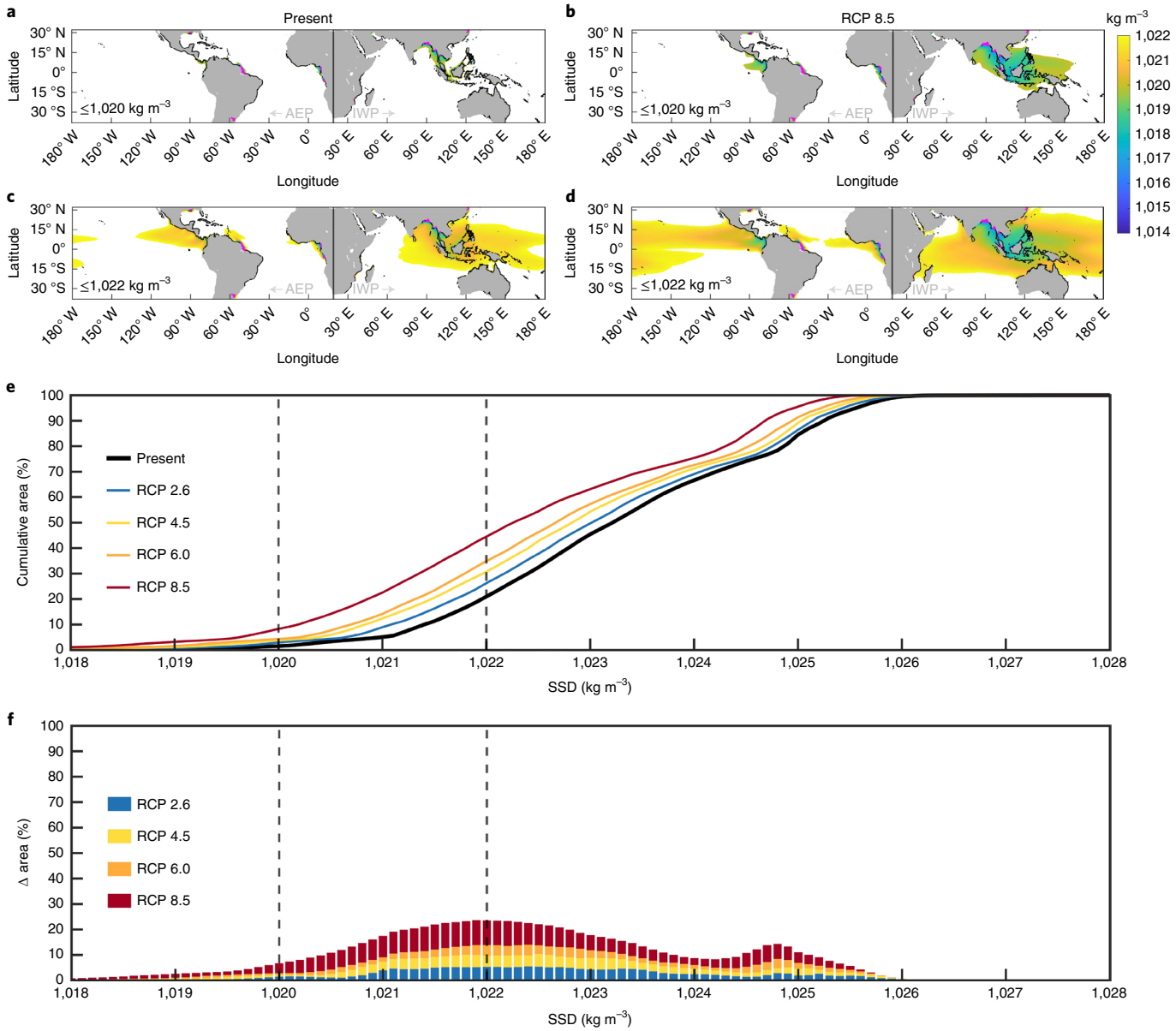

Fig. 5 | Future changes in SSD. a–d, Spatial extent of coastal and open-ocean surface waters with a density ≤1,020 kg m^{-3} (**a**,**b**) and 1,022 kg m^{-3} (**c**,**d**), for present (2000–2014) (**a**,**c**) and future (2090–2100; RCP 8.5) (**b**,**d**) scenarios. Data are shown for surface ocean waters within the global latitudinal range of mangrove forests (between 32° N and 38° S). The two density thresholds considered are within the range of densities at which mangrove propagule buoyancy and floating orientation of several mangrove genera change, as reported in available literature. Black dots along the coast represent the global mangrove extent from the 2015 GMW dataset[32]. Magenta-coloured circles represent SSD values <1,014 kg m^{-3}. **e**,**f**, Ocean area with a density less than or equal to SSD (**e**) and future changes in the spatial extent of these regions (**f**) for different RCP scenarios.

mangrove propagule dispersal, we considered threshold water density values (1,020 and 1,022 kg m^{-3}) that are within the range where elongated propagules of important mangrove genera tend to change floating orientation (Fig. 4a). More specifically, we determined the ocean surface area with an SSD below or equal to these thresholds under different climate change scenarios (Fig. 5). Under RCP 8.5, the ocean surface covered by mangrove coastal waters (coastal waters bordering present mangrove forests) with a density ≤1,020 kg m^{-3} increases ~27% by 2100, notably more so in the IWP (~37%) than in the AEP (~6%) (Supplementary Table 6). A threshold of 1,022 kg m^{-3} results in increases of roughly +11% (global), +12% (IWP) and +8% (AEP) (Supplementary Table 7). Similar spatial patterns are observed for open-ocean waters within the global latitudinal range of mangroves (Fig. 5 and Supplementary Figs. 1 and 2).

Our study shows changes in the physical and chemical properties of coastal mangrove waters by the end of the twenty-first century that could affect the distribution of propagules from widespread mangrove genera (*Avicennia*, *Bruguiera*, *Ceriops* and *Rhizophora*) and probably more so within the IWP region, the primary hotspot of mangrove diversity, compared to the AEP. Propagules from these genera have densities that are close to that of seawater and experimental evidence shows that propagules in species of these genera typically become denser as they age[36–39]. For mangroves in large parts of the IWP, as well as the Gulf of Guinea in the AEP, declines in SSD could therefore promote local sinking rates and reduce the probability of successful long-distance dispersal due to earlier propagule sinking before reaching suitable establishment zones (Fig. 4). Indeed, future changes in surface ocean proper-

ties may impact dispersal differently at different scales. More specifically, short-distance dispersal may be promoted and successful long-distance dispersal reduced since (1) freshening of local waters near the propagule release site and associated sinking can reduce the fraction of propagules reaching open-ocean waters; and (2) older propagules that have travelled longer distances are at risk of offshore sinking due to the combined effect of increased propagule density during transport[36–39] and fresher coastal waters; as such, increased ocean freshening and warming and resulting changes in SSD are likely to reduce the tail of the dispersal kernel—which captures long-distance dispersal events. Upon sinking, a propagule is at least temporarily eliminated from the dispersing cohort and prone to mortality associated with stranding in unsuitable conditions. Empirical evidence of mangrove distributions limited by sinking of propagules under increasingly fresher conditions in estuaries was shown for mangroves along the Nakara River in Japan[36]. Such effects are of considerable importance, since some of the most pronounced changes in SSS and SSD are near major river outlets where many of the most extensive mangrove areas in the world are found[1], such as the Ganges–Brahmaputra delta. In contrast to the wide-ranging mangrove genera *Avicennia*, *Bruguiera*, *Ceriops* and *Rhizophora*, mangrove species such as *H. littoralis* and *Xylocarpus granatum* are unlikely to be affected by these ocean changes as their propagules possess very low densities[13].

An additional level of complexity is that the floating orientation of propagules from several widespread mangrove genera (*Rhizophora* and *Ceriops*) could move between horizontal and vertical due to small changes in density[38,40,41]. Changes in floating orientation have been associated with the replacement of air in intercellular tissue by water via lenticels[38]; however, while the exact anatomical and physiological mechanisms underlying changes in mangrove propagule buoyancy are not yet fully understood, experimental and modelling studies showed that these changes in floating orientation can strongly alter dispersal trajectories at the landscape (10^2–10^3 m), regional (10^3–10^5 m), as well as the biogeographic scale (10^5–10^7 m), via the relative effects of ocean and wind forces on propagule transport[42–44].

Besides effects of changes in SSD, propagule dispersal may also be directly impacted by SSS or SST. In *Avicennia marina*, propagule sinking has been associated with the shedding of the pericarp (Steinke, 1975, as cited in ref. [45]) and the time required for pericarp shedding and the separation of the cotyledons increases with increasing salinity (Downton, 1982, as cited in ref. [45]). As such, future ocean freshening might decrease floating periods and potentially dispersal distances in this species. Increases in SSS might also result in higher propagule mortality rates and lower germination success[40], whereas lower SSS could reduce propagule viability by increasing the incidence of fungal infestation and rotting[46]. Finally, projected increases in SST may facilitate mangrove expansion to higher latitudes in some regions by reducing the negative effect of colder oceanic waters on propagule viability[47]. For example, an earlier study on the western South Atlantic latitudinal mangrove range limit reported that temperatures <20 °C may limit the viability of mangrove propagules during their dispersal along this coast and during subsequent establishment[48]. However, since empirical data on potential direct effects of SSS and SST on mangrove propagule dispersal are deficient, effects of these variables require further investigation.

It is important to note that changes indicated by our study are based on changes in time-mean surface ocean properties and that the actual variability in SSD around these mean values could be higher. Since mangroves thrive in a broad range of coastal settings, including estuaries, deltas, lagoons and open coast, their propagules already encounter a wide range of water densities today but our findings clearly illustrate that for important mangrove regions worldwide exposure to lower-density waters will occur more frequently in the future. While our results suggest changes in dispersal patterns following climate-driven changes in coastal and open-ocean surface-water properties, the effects also depend on adaptive capacity. Under current ocean conditions, propagule densities that are just slightly lower than that of seawater are probably adaptive, since this ensures that they sink in favourable coastal environments, that is, along coastal zones where SSS and SSD are lower due to freshwater influx from rivers. Yet, in future oceans the spatial extent of these lower-density waters may expand further offshore, altering buoyancy characteristics and the spatial distribution of propagules. The demographic costs associated with ending up in unsuitable habitat (for example, due to offshore sinking) can get balanced when populations evolve to have lower propagule densities. As such, there is a need for quantitative data for inter- and intra-population variation in the critical SSD at which mangrove propagules sink, which could reflect underlying genetic variation in propagule density that can fuel evolutionary change. Overall, our results suggest that we may be entering a density-induced transition phase as part of the Anthropocene, highlighting the importance of considering future ocean property changes in evaluating the impacts of climate change on mangrove ecosystems. Such information will complement knowledge on the effects of other impacting factors and is important for predicting how altered environmental conditions will affect these sensitive forests. Finally, while we considered mangroves as a model system in this study, our findings may be relevant also for other coastal taxa producing sea-drifted propagules, such as seagrasses[49] and coastal strand communities (*Terminalia catappa*, *Barringtonia asiatica*, *Thespesia populnea*, *Hibiscus tiliaceus*, *Pisonia grandis*, *Pandanus* spp. and so on).

Online content

Any methods, additional references, Nature Research reporting summaries, source data, extended data, supplementary information, acknowledgements, peer review information; details of author contributions and competing interests; and statements of data and code availability are available at https://doi.org/10.1038/s41558-022-01391-9.

Received: 8 October 2021; Accepted: 13 May 2022;
Published online: 30 June 2022

References

1. Spalding, M., Kainuma, M. & Collins, L. *World Atlas of Mangroves* (Earthscan and James & James, 2010).
2. Barbier, E. B. et al. The value of estuarine and coastal ecosystem services. *Ecol. Monogr.* **81**, 169–193 (2011).
3. Ellison, J. Vulnerability assessment of mangroves to climate change and sea-level rise impacts. *Wetl. Ecol. Manag.* **23**, 115–137 (2015).
4. Ward, R. D., Friess, D. A., Day, R. H. & MacKenzie, R. A. Impacts of climate change on mangrove ecosystems: a region by region overview. *Ecosyst. Health Sust.* **2**, e01211 (2016).
5. Saintilan, N. et al. Mangrove expansion and salt marsh decline at mangrove poleward limits. *Glob. Change Biol.* **20**, 147–157 (2014).
6. Cavanaugh, K. C. et al. Poleward expansion of mangroves is a threshold response to decreased frequency of extreme cold events. *Proc. Natl Acad. Sci. USA* **111**, 723–727 (2014).
7. Kelleway, J. J. et al. Review of the ecosystem service implications of mangrove encroachment into salt marshes. *Glob. Change Biol.* **23**, 3967–3983 (2017).
8. Pecl, T. P. et al. Biodiversity redistribution under climate change: impacts on ecosystems and human well-being. *Science* **355**, 1389 (2017).
9. Osland, M. J. et al. Climatic controls on the global distribution, abundance, and species richness of mangrove forests. *Ecol. Monogr.* **87**, 341–359 (2017).
10. Thom, B. G. Mangrove ecology and deltaic geomorphology: Tabasco, Mexico. *J. Ecol.* **55**, 301–343 (1967).
11. Duke, N. C., Ball, M. C. & Ellison, J. C. Factors influencing biodiversity and distributional gradients in mangroves. *Glob. Ecol. Biogeogr. Lett.* **7**, 27–47 (1998).
12. Raw, J. L., Godbold, J. A., van Niekerk, L. & Adams, J. B. Drivers of mangrove distribution at the high-energy, wave-dominated, southern African range limit. *Estuar. Coast. Shelf Sci.* **226**, 106296 (2019).

13. Van der Stocken, T. et al. A general framework for propagule dispersal in mangroves. *Biol. Rev.* **94**, 1547–1575 (2019).
14. Cavanaugh, K. C. et al. Climate-driven regime shifts in a mangrove–salt marsh ecotone over the past 250 years. *Proc. Natl Acad. Sci. USA* **116**, 21602–21608 (2019).
15. Woodroffe, C. D. & Grindrod, J. Mangrove biogeography: the role of Quaternary environmental and sea-level change. *J. Biogeogr.* **18**, 479–492 (1991).
16. Hoppe-Speer, S. C. L., Adams, J. B. & Rajkaran, A. Mangrove expansion and population structure at a planted site, East London, South Africa. *South. For.* **77**, 131–139 (2015).
17. Van der Stocken, T. et al. Global-scale dispersal and connectivity in mangroves. *Proc. Natl Acad. Sci. USA* **116**, 915–922 (2019).
18. Guppy, H. B. *Observations of a Naturalist in the Pacific Between 1896 and 1899: Plant Dispersal* Vol. II (Macmillan and Co., 1906).
19. Bindoff, N. L. et al. in *Special Report on the Ocean and Cryosphere in a Changing Climate* (eds Pörtner, H.-O. et al.) 447–587 (WMO, 2019).
20. Johnson, G. C. & Wijffels, S. E. Ocean density change contributions to sea level rise. *Oceanography* **24**, 112–121 (2011).
21. Alongi, D. M. The impact of climate change on mangrove forests. *Curr. Clim. Change Rep.* **1**, 30–39 (2015).
22. Lovelock, E. C. et al. The vulnerability of Indo-Pacific mangrove forests to sea-level rise. *Nature* **526**, 559–563 (2015).
23. Osland, M. J. et al. Mangrove forests in a rapidly changing world: global change impacts and conservation opportunities along the Gulf of Mexico coast. *Estuar. Coast. Shelf Sci.* **214**, 120–140 (2018).
24. O'Connor, M. I. et al. Temperature control of larval dispersal and the implications for marine ecology, evolution, and conservation. *Proc. Natl Acad. Sci. USA* **104**, 1266–1271 (2007).
25. Wilson, L. J. et al. Climate-driven changes to ocean circulation and their inferred impacts on marine dispersal patterns. *Glob. Ecol. Evol.* **25**, 923–939 (2016).
26. Poloczanska, E. S. et al. Responses of marine organisms to climate change across oceans. *Front. Mar. Sci.* **3**, 62 (2016).
27. Pinsky, M. L., Eikeset, A. M., McCauley, D. J., Payne, J. L. & Sunday, J. M. Greater vulnerability to warming of marine versus terrestrial ectotherms. *Nature* **569**, 108–111 (2019).
28. Spalding, M. D. et al. Marine ecoregions of the world: a bioregionalization of coastal and shelf areas. *BioScience* **57**, 573–583 (2007).
29. Tyberghein, L. et al. Bio-ORACLE: a global environmental dataset for marine species distribution modelling. *Glob. Ecol. Biogeogr.* **21**, 272–281 (2012).
30. Assis, J. et al. Bio-ORACLE v2.0: extending marine data layers for bioclimatic modelling. *Glob. Ecol. Biogeogr.* **27**, 277–284 (2017).
31. Fofonoff, P. & Millard, R. C. Algorithms for computation of fundamental properties of seawater. *UNESCO Techn. Papers in Mar. Sci.* **44** (UNESCO, 1983).
32. Bunting, P. et al. The Global Mangrove Watch—a new 2010 global baseline of mangrove extent. *Remote Sens.* **10**, 1669 (2018).
33. Bruno, J. F. et al. Climate change threatens the world's marine protected areas. *Nat. Clim. Change* **8**, 499–503 (2018).
34. Moon, S. & Ha, K. J. Future changes in monsoon duration and precipitation using CMIP6. *Clim. Atmos. Sci.* **3**, 45 (2020).
35. Durack, P. J. & Wijffels, S. E. Fifty-year trends in global ocean salinities and their relationship to broad-scale warming. *J. Clim.* **23**, 4342–4362 (2010).
36. Kadoya, T. & Inoue, T. Spatio-temporal pattern of specific gravity of mangrove diaspore: implications for upstream dispersal. *Ecography* **38**, 472–479 (2015).
37. Robert, E. M. R. et al. Viviparous mangrove propagules of *Ceriops tagal* and *Rhizophora mucronata*, where both Rhizophoraceae show different dispersal and establishment strategies. *J. Exp. Mar. Bio. Ecol.* **468**, 45–54 (2015).
38. Tonné, N., Beeckman, H., Robert, E. M. R. & Koedam, N. Towards an unknown fate: the floating behaviour of recently abscised propagules from wide ranging Rhizophoraceae mangrove species. *Aquat. Bot.* **140**, 23–33 (2017).
39. Wang, W., Li, X. & Wang, M. Propagule dispersal determines mangrove zonation at intertidal and estuarine scales. *Forests* **10**, 245 (2019).
40. Rabinowitz, D. Dispersal properties of mangrove propagules. *Biotropica* **10**, 47–57 (1978).
41. Clarke, P. J., Kerrigan, R. A. & Westphal, C. J. Dispersal potential and early growth in 14 tropical mangroves: do early life history traits correlate with patterns of adult distribution? *J. Ecol.* **89**, 648–659 (2001).
42. Van der Stocken, T. et al. The role of wind in hydrochorous mangrove propagule dispersal. *Biogeosciences* **10**, 3635–3647 (2013).
43. Van der Stocken, T. et al. Interaction between water and wind as a driver of passive dispersal in mangroves. *PLoS ONE* **10**, e0121593 (2015).
44. Van der Stocken, T. & Menemenlis, D. Modelling mangrove propagule dispersal trajectories using high-resolution estimates of ocean surface winds and currents. *Biotropica* **49**, 472–481 (2017).
45. Hutchings, P. & Saenger, P. *The Ecology of Mangroves* (Univ. of Queensland Press, 1987).
46. Alleman, L. K. & Hester, M. W. Reproductive ecology of black mangrove (*Avicennia germinans*) along the Louisiana coast: propagule production cycles, dispersal limitations, and establishment elevations. *Estuar. Coast.* **34**, 1068–1077 (2011).
47. Hickey, M. H. et al. Is climate change shifting the poleward limit of mangroves?. *Estuar. Coast* **40**, 1215–1226 (2017).
48. Soares, M. L. G., Estrada, G. C. D. E., Fernandez, V. & Tognella, M. M. P. Southern limit of the western South Atlantic mangroves: assessment of the potential effects of global warming from a biogeographical perspective. *Estuar. Coast. Shelf Sci.* **101**, 44–53 (2012).
49. Repolho, T. et al. Seagrass ecophysiological performance under ocean warming and acidification. *Sci. Rep.* **7**, 41443 (2017).
50. Allen, M. et al. Raincloud plots: a multi-platform tool for robust data visualization (version 2). *Wellcome Open Res.* **4**, 63 (2021).
51. Van der Stocken, T., Vanschoenwinkel, B., De Ryck, D. & Koedam, N. Caught in transit: offshore interception of seafaring propagules from seven mangrove species. *Ecosphere* **9**, e02208 (2018).

Methods

Ocean data. In this study we examine changes in SST, SSS and SSD over the next century. SSD has been largely overlooked in studies that examine the response of marine organisms to climate-driven ocean changes, despite its potential influence on the dispersal patterns and colonization potential of passive propagules with near-seawater densities. We calculated changes in mean SST and SSS over the next century using present (2000–2014) and future (2090–2100) data from Bio-ORACLE[29,30], a database of GIS rasters providing geophysical, biotic and environmental data for surface and benthic marine realms (https://www.bio-oracle.org/). These data consist of uniformly constructed rasters provided at a spatial resolution of 5 arcmin (~0.08° or ~9.2 km at the Equator). Present layers were generated with climate data describing monthly means for the period 2000–2014, acquired from preprocessed global ocean ARMOR reanalyses that combine remotely sensed and in situ observations, while future data were produced by averaging output from atmosphere–ocean general circulation models provided by the Coupled Model Intercomparison Project Phase 5 (CMIP5)[30]. We are aware of the limitations of remotely sensed coastal ocean data and climate change projections of fine-scale near-shore circulation patterns, which may deviate from in situ observations[52]. However, using time-averaged SST and SSS data and considering spatially averaged patterns ensures that we are capturing general trends in coastal ocean changes. SSD was derived from these variables using the UNESCO EOS-80 equation of state polynomial for seawater[31]. Changes were calculated for four RCP scenarios: RCP 2.6 (490 CO_2e before 2100 and then decline), RCP 4.5 (650 CO_2e at stabilization after 2100), RCP 6.0 (850 CO_2e at stabilization after 2100) and RCP 8.5 (>1,370 CO_2e in 2100) (see ref. [53] for more details about RCPs).

Global mangrove range data. The GMW provides high-resolution (0.8 arcsec or ~25 m) global mangrove extent baseline maps based on Landsat sensor spectral composite data and Advanced Land Observing Satellite (ALOS) Phased Arrayed L-band Synthetic Aperture Radar (PALSAR) data for the years 1996, 2007, 2008, 2009, 2010, 2015 and 2016 (ref. [32]). For this study, we used the 2015 mangrove extent baseline map since it most closely matches the end year of the period (2000–2014) considered for generating the Bio-ORACLE raster data of present-day marine environmental conditions[30]. Using the QGIS 3.10.10 software, centroids were computed for each GMW 2015 polygon (n = 583,578) and considered as our global mangrove occurrence dataset. Global mangrove occurrence points were assigned to the nearest grid cell (Euclidean distance) in the Bio-ORACLE fields. Since multiple occurrence points might have been assigned to the same grid cell, duplicates were removed, resulting in unique grid cell records for the GMW 2015 mangrove range (n = 10,108). Each of these steps was performed using the MATLAB 2020b programming software.

Mangrove species-specific data. A literature survey was conducted to collect data on mangrove propagule density values that were interpreted against the range of present and future SSD values within the range of *Avicennia germinans* (AEP), *Avicennia marina* (IWP), *Bruguiera gymnorrhiza* (IWP), *Ceriops tagal* (IWP), *Heritiera littoralis* (IWP), *Rhizophora mangle* (AEP), *Rhizophora mucronata* (IWP) and *Xylocarpus granatum* (IWP). This selection of mangrove species in our literature survey is based on the availability of propagule density data. Such data are surprisingly limited but nevertheless allow for a first assessment of species-specific differences in the sensitivity to SSD changes. Additionally, propagules of the selected species are representative for the variety of propagule morphotypes found among mangrove species globally and include the most widely distributed mangrove species (*Avicennia* spp. and *Rhizophora* spp.) for which distributional changes have been reported and predicted[5,54,55]. In the case that specific gravity values were reported[36,56], we multiplied these values by 999.97 kg m^{-3} (the density of water at 4 °C, which is the standard density used to compute specific gravity) to obtain density values.

The 2015 GMW database used for our global analysis does not contain coordinates for species-specific mangrove distributions. Hence, data for different species were generated using vector layers obtained from the IUCN Red List website (https://www.iucnredlist.org/). The IUCN data for each species consist of a single polygon feature that was intersected with a 1:10 m global coastline downloaded from the Natural Earth database (https://www.naturalearthdata.com/) in QGIS 3.10.10. Before this intersection, we buffered the species distribution polygons using a buffer distance equal to the spatial resolution of the Bio-ORACLE marine data layers (0.5 arcmin) to avoid losing data where the original IUCN species distribution polygons did not overlap with the global coastline data. Point features were generated at 1 km distance for each line feature representing a species range, using the QChainage plugin in QGIS 3.10.10 and longitude and latitude information was added to each point for *A. germinans* (n = 4,610), *A. marina* (n = 11,231), *B. gymnorrhiza* (n = 9,665), *C. tagal* (n = 9,134), *H. littoralis* (n = 7,984), *R. mangle* (n = 3,431), *R. mucronata* (n = 9,519) and *X. granatum* (n = 8,890). Since the IUCN data show mangrove presence along vast stretches of coast (for example, Somalia and East Madagascar) where mangroves are absent in the 2015 GMW data, we extracted ocean data for the IUCN coordinates that correspond with a 2015 GMW occurrence point (the centroids of each 2015 GMW polygon feature). The resulting coordinates for *A. germinans* (n = 2,964), *A. marina* (n = 6,419), *B. gymnorrhiza* (n = 6,040), *C. tagal* (n = 5,653), *H. littoralis* (n = 5,100), *R. mangle* (n = 2,345), *R. mucronata* (n = 5,348) and *X. granatum* (n = 5,891) can be viewed as species-specific GMW data. Each of these computations was performed using the MATLAB 2020b programming software.

Spatial analyses. Spatial patterns in projected ocean property changes over the next century were explored by considering bioregion- and province-levels to subset our GMW 2015 data. Bioregion subsetting consists of coastal Bio-ORACLE cells in the AEP (between −180° and 19° longitude) and IWP (between 19° and 180° longitude) bioregion, whereas the province-level waters consist of a subsetting using the provinces provided by the MEOW dataset[28].

Reporting summary. Further information on research design is available in the Nature Research Reporting Summary linked to this article.

Data availability

All the datasets used for analyses during this study are publicly available and can be accessed at: https://www.bio-oracle.org/ (marine data layers[29,30]); https://data.unep-wcmc.org/datasets/45 (global mangrove extent[32]); https://www.iucnredlist.org/ (geographic range of the species considered); https://data.unep-wcmc.org/datasets/38 (provinces from the MEOW database[28]). All remaining data that support the findings of this study are freely available at https://doi.org/10.5061/dryad.66t1g1k4c (ref. [57]).

Code availability

Computations of SSD were conducted using the UNESCO EOS-80 equation of state polynomial for seawater (*sw_dens.m* from the MATLAB seawater package)[31]. Other MATLAB codes used during the current study are available from the corresponding author upon reasonable request.

References

52. Smit, J. S. et al. A coastal seawater temperature dataset for biogeographic studies: large biases between *in situ* and remotely-sensed data sets around the coast of South Africa. *PLOS ONE* **8**, e81944 (2013).
53. Moss, R. et al. The next generation of scenarios for climate change research and assessment. *Nature* **463**, 747–756 (2010).
54. Quisthoudt, K. et al. Disentangling the effects of global climate and regional land-use change on the current and future distribution of mangroves in South Africa. *Biodivers. Conserv.* **22**, 1369–1390 (2013).
55. Cavanaugh, K. C. et al. Sensitivity of mangrove range limits to climate variability. *Glob. Ecol. Biogeogr.* **27**, 925–935 (2018).
56. McKee, L. K. Seedling recruitment patterns in a Belizean mangrove forest: effects of establishment ability and physico-chemical factors. *Oecologia* **101**, 448–460 (1995).
57. Van der Stocken, T. et al. Future changes in mangrove coastal water properties. *Dryad* https://doi.org/10.5061/dryad.66t1g1k4c (2022).

Acknowledgements

T.V.d.S. is supported by the EU Horizon 2020 Framework Programme for Research and Innovation under the Marie Skłodowska-Curie actions Individual Fellowship (MSCA-IF) with grant agreement no. 896888 (GLOMAC). K.C.C. is supported by the NASA Land Cover and Land Use Change (LCLUC) Program with grant no. 80NSSC21K0296.

Author contributions

T.V.d.S. designed the study, compiled and analysed the data, produced the figures, interpreted the results and wrote the manuscript with contributions and suggestions from B.V., D.C., K.C. and N.K. T.V.d.S and D.C. computed sea surface density fields. B.V. provided extensive feedback on various drafts and revisions of the manuscript.

Competing interests

The authors declare no competing interests.

Additional information

Supplementary information The online version contains supplementary material available at https://doi.org/10.1038/s41558-022-01391-9.

Correspondence and requests for materials should be addressed to Tom Van der Stocken.

Peer review information *Nature Climate Change* thanks Ken Krauss, Erik Yando and the other, anonymous, reviewer(s) for their contribution to the peer review of this work.

nature portfolio

Corresponding author(s): Tom Van der Stocken

Last updated by author(s): May 5, 2022

Reporting Summary

Nature Portfolio wishes to improve the reproducibility of the work that we publish. This form provides structure for consistency and transparency in reporting. For further information on Nature Portfolio policies, see our Editorial Policies and the Editorial Policy Checklist.

Statistics

For all statistical analyses, confirm that the following items are present in the figure legend, table legend, main text, or Methods section.

n/a	Confirmed
☒	☐ The exact sample size (*n*) for each experimental group/condition, given as a discrete number and unit of measurement
☒	☐ A statement on whether measurements were taken from distinct samples or whether the same sample was measured repeatedly
☒	☐ The statistical test(s) used AND whether they are one- or two-sided *Only common tests should be described solely by name; describe more complex techniques in the Methods section.*
☒	☐ A description of all covariates tested
☒	☐ A description of any assumptions or corrections, such as tests of normality and adjustment for multiple comparisons
☒	☐ A full description of the statistical parameters including central tendency (e.g. means) or other basic estimates (e.g. regression coefficient) AND variation (e.g. standard deviation) or associated estimates of uncertainty (e.g. confidence intervals)
☒	☐ For null hypothesis testing, the test statistic (e.g. *F*, *t*, *r*) with confidence intervals, effect sizes, degrees of freedom and *P* value noted *Give P values as exact values whenever suitable.*
☒	☐ For Bayesian analysis, information on the choice of priors and Markov chain Monte Carlo settings
☒	☐ For hierarchical and complex designs, identification of the appropriate level for tests and full reporting of outcomes
☒	☐ Estimates of effect sizes (e.g. Cohen's *d*, Pearson's *r*), indicating how they were calculated

Our web collection on statistics for biologists contains articles on many of the points above.

Software and code

Policy information about availability of computer code

Data collection	All the datasets used for analyses during this study are publicly available and can be accessed at: https://www.bio-oracle.org/ (marine data layers); https://data.unep-wcmc.org/datasets/45 (global mangrove extent); https://www.iucnredlist.org/ (geographic range of the mangrove species considered); https://data.unep-wcmc.org/datasets/38 (provinces from the Marine Ecoregions of the World database). Data extraction was performed using the QGIS 3.10.10 software, which can be downloaded from https://download.qgis.org/downloads/.
Data analysis	Computations of SSD were conducted using the UNESCO EOS-80 equation of state polynomial for seawater ('sw_dens' from the MATLAB seawater package; Fofonoff, P. & Millard, R. C. Algorithms for computation of fundamental properties of seawater. UNESCO Techn. Papers in Mar. Sci. 44 (UNESCO, 1983)). Data analysis was performed using our own computer codes using the MATLAB 2020b programming software. Maps in Figs. 1, 2, 5a, 5b, 5c, and 5d, were generated using the Matlab Mapping Toolbox. Cat-eye plots in Fig. 2 were generated using the visualization approach from Allen et al. (2019): Raincloud plots: a multi-platform tool for robust data visualization (version 2). Wellcome Open Res 4, 63 (2021). Schematic figures in Fig. 4 (panel b and bottom part of panel a) were generated using the PowerPoint software v.16.60.

For manuscripts utilizing custom algorithms or software that are central to the research but not yet described in published literature, software must be made available to editors and reviewers. We strongly encourage code deposition in a community repository (e.g. GitHub). See the Nature Portfolio guidelines for submitting code & software for further information.

Data

Policy information about availability of data

All manuscripts must include a data availability statement. This statement should provide the following information, where applicable:

- Accession codes, unique identifiers, or web links for publicly available datasets
- A description of any restrictions on data availability
- For clinical datasets or third party data, please ensure that the statement adheres to our policy

Global mangrove occurrence data (longitude, latitude) generated and used here, as well as the extracted ocean-surface property data for present and future climate scenarios, have been deposited into the Dryad data repository (doi:10.5061/dryad.66t1g1k4c). Reported mangrove propagule density values compiled from the literature and used here, are provided as Supplementary Table 5. There are no restrictions on data usage and access.

Field-specific reporting

Please select the one below that is the best fit for your research. If you are not sure, read the appropriate sections before making your selection.

☐ Life sciences ☐ Behavioural & social sciences ☒ Ecological, evolutionary & environmental sciences

For a reference copy of the document with all sections, see nature.com/documents/nr-reporting-summary-flat.pdf

Ecological, evolutionary & environmental sciences study design

All studies must disclose on these points even when the disclosure is negative.

Study description	Using global surface ocean data from the Bio-ORACLE database (spatial resolution: 5 arcmin, which is ca. 0.08° or 9.2 km at the equator) and mangrove distributional data from the Global Mangrove Watch, we calculated future (2090–2100) changes in sea-surface density (coastal waters) across the global range of mangrove, for four representative concentration pathways (RCPs), investigating spatial patterns using the Marine Ecoregions of the World data, and among the world's two major mangrove biogeographical regions: the Atlantic East Pacific (AEP), including all of the Americas, West and Central Africa, and the Indo-West Pacific (IWP), extending from East Africa eastwards to the islands of the central Pacific.
Research sample	Our study focuses on the global mangrove range and 8 different mangrove species, and considers present (2000-2014) and future (2090-2100) surface-ocean variables for four representative concentration pathways (RCPs). The global dataset includes 10108 entries. Other datasets are for 8 mangrove species that collectively cover the two major mangrove biogeographical regions: the Atlantic East Pacific (AEP), including all of the Americas, West and Central Africa, and the Indo-West Pacific (IWP), extending from East Africa eastwards to the islands of the central Pacific. Selected species are the following: Avicennia germinans (AEP, 2964 entries), Avicennia marina (IWP, 6419 entries), Bruguiera gymnorrhiza (IWP, 6040 entries), Ceriops tagal (IWP, 5653 entries), Heritiera littoralis (IWP, 5100 entries), Rhizophora mangle (AEP, 2345 entries), Rhizophora mucronata (IWP, 5348 entries), and Xylocarpus granatum (IWP, 5891 entries).
Sampling strategy	Besides the global mangrove range, we also selected 8 mangrove species. The selection of these species is based on the following rationale: (1) they collectively cover the two major mangrove biogeographical regions; (2) available propagule density data for mangrove species in the literature; (3) propagules of these species are representative for the variety of propagule morphotypes found among mangrove species globally and include the most widely-distributed mangrove species (i.e., Avicennia spp. and Rhizophora spp.).
Data collection	Data were collected, extracted, compiled and analysed by Dr. Tom Van der Stocken. Sea-surface density fields were computed by Dr. Tom Van der Stocken and Dr. Dustin Carroll.
Timing and spatial scale	The study considers changes in sea-surface temperature, sea-surface salinity and sea-surface density in the 21st century, i.e., between present (2000-2014) and future (2090-2100). Spatially, the study considers three levels: (1) global (global mangrove distribution as in the 2015 Global Mangrove Watch data); (2) the world's two major mangrove diversity hotspots: Atlantic East Pacific (AEP, between -180 and 19 degrees longitude) and Indo-West Pacific (IWP, between 19 and 180 degrees longitude); and (3) province-level waters obtained by sub-setting the data using the provinces provided by the Marine Ecoregions of the World (MEOW) dataset from Spalding et al. (2007, Marine ecoregions of the world: A bioregionalization of coastal and shelf areas. BioScience 57, 573–583).
Data exclusions	Our study focuses on open-ocean and coastal waters within the latitudinal limits of the global mangrove range. Hence, other coastal stretches are excluded from our study. Regarding mangrove species, the focus is on widely-distributed mangrove species for which propagule density values are reported in the literature. Other mangrove species were not considered.
Reproducibility	The study consists of computational analysis of public data, and hence, is highly reproducible.
Randomization	Data randomization is not relevant to our study. Data were grouped according to spatially delineated areas (existing classifications: bioregions, ecoprovinces, species-level polygons) and does not comprise experimental data.
Blinding	Blinding is not applicable to our computations because the same code/approach will generate the same results on other computing platforms.

Did the study involve field work? ☐ Yes ☒ No

Reporting for specific materials, systems and methods

We require information from authors about some types of materials, experimental systems and methods used in many studies. Here, indicate whether each material, system or method listed is relevant to your study. If you are not sure if a list item applies to your research, read the appropriate section before selecting a response.

Materials & experimental systems

n/a	Involved in the study
☒	☐ Antibodies
☒	☐ Eukaryotic cell lines
☒	☐ Palaeontology and archaeology
☒	☐ Animals and other organisms
☒	☐ Human research participants
☒	☐ Clinical data
☒	☐ Dual use research of concern

Methods

n/a	Involved in the study
☒	☐ ChIP-seq
☒	☐ Flow cytometry
☒	☐ MRI-based neuroimaging